Applied Surface Science 258 (2012) 10135–10139

Contents lists available at SciVerse ScienceDirect

Applied Surface Science

journal homepage: www.elsevier.com/locate/apsusc

Magnetic and electronic properties of silicane with hydrogen vacancies on the surface

L. Pan [a], H.J. Liu [a,*], Y.W. Wen [a], X.J. Tan [a], H.Y. Lv [a], J. Shi [a], X.F. Tang [b]

[a] Key Laboratory of Artificial Micro- and Nano-structures of Ministry of Education and School of Physics and Technology, Wuhan University, Wuhan 430072, China
[b] State Key Laboratory of Advanced Technology for Materials Synthesis and Processing, Wuhan University of Technology, Wuhan 430070, China

ARTICLE INFO

Article history:
Received 29 April 2012
Received in revised form 5 June 2012
Accepted 24 June 2012
Available online 2 July 2012

Keywords:
Silicane
First-principles
Surface vacancies
Magnetic properties
Electronic properties

ABSTRACT

By using first-principles pseudopotential calculations, we investigate the magnetic and electronic properties of hydrosilicon honeycomb structure (silicane) with hydrogen vacancies on its surface. It is found that a single vacancy created on the nonmagnetic silicane can induce a magnetic moment of one μ_B. When a domain of vacancies is considered, the magnetization is determined by the size and geometry of the domain, and whether it is single- or double-sided. Compared with the energy band structure of silicane, the creation of domain causes very flat bands around the Fermi level and tends to reduce the band gap. It is interesting to find that the systems with single-sided domain all exhibit a band gap of about 1.0 eV while those of double-sided domain exhibit strong size dependence.

1. Introduction

Since the pioneering fabrication of graphene by mechanical exfoliation of graphite [1], this two-dimensional honeycomb structure of carbon has been the subject of intensive studies because of its versatile electronic properties [2–6]. A graphene can be made magnetic by cutting it into nanoribbons with varying widths and edges [5,7–10] or by the presence of topological defects [11–14]. Recently, a hydrocarbon derivative of graphene called graphane was synthesized by direct exposure to H_2 plasma, and the reversible hydrogenation–dehydrogenation with changing temperature has been revealed [15]. In addition to their interesting electronic properties [16–20], magnetism can be obtained in the graphane with domain of surface hydrogen vacancies [21–23]. It therefore provides a practical alternative to graphene nanoribbons where magnetic moment only appears in the zigzag edges, or graphene with defects where the integrity of honeycomb structure is destroyed.

The rapid raise of graphene research has stimulated a lot of work to investigate the honeycomb lattices of other group IV elements. For example, it was theoretically predicated that silicon honeycomb structure (silicene) with a puckered geometry could be stable, and the corresponding electronic properties is similar to that of graphene [24–28]. Moreover, it is found that a vertical electric field can open a band gap in semimetallic silicene [29]. Indeed, the graphene-like structure of silicon has been experimentally synthesized through epitaxial growth on a close-packed silver surface [30]. Compared with graphene, the integration of silicene into Si-based nanoelectronics would be more favorable. Very recently, the electronic structures of completely hydrogenated silicene (silicane) has also been predicated [31–34]. To see if controllable magnetism can be obtained in the two-dimensional silicon materials, in this work, we focus on the so-called silicane with hydrogen vacancies on its surfaces. Such kinds of structure are very similar to the graphane counterpart, but have different magnetic and electronic properties according to our first-principles calculations.

2. Computational details

Our calculations have been performed by using a plane-wave pseudopotential formulation [35–37] within the framework of density functional theory (DFT). The code is implemented in the Vienna ab initio simulation package (VASP). We use ultrasoft pseudopotentials for the silicon and hydrogen atoms, and the exchange-correlation energy is in the form of Perdew-Wang-91 [38]. The silicane structure with surface hydrogen vacancies is modeled by using a $6 \times 6 \times 1$ supercell geometry where the closest distance between the Si layer and its periodic image is set to 10 Å. At such a separation, the layer-layer interactions are very small so that they can be treated as independent entities. The plane-wave cutoff is set to 200 eV, and the Brillouin zone is sampled with

* Corresponding author.
E-mail address: phlhj@whu.edu.cn (H.J. Liu).

0169-4332/$ – see front matter © 2012 Elsevier B.V. All rights reserved.
http://dx.doi.org/10.1016/j.apsusc.2012.06.092

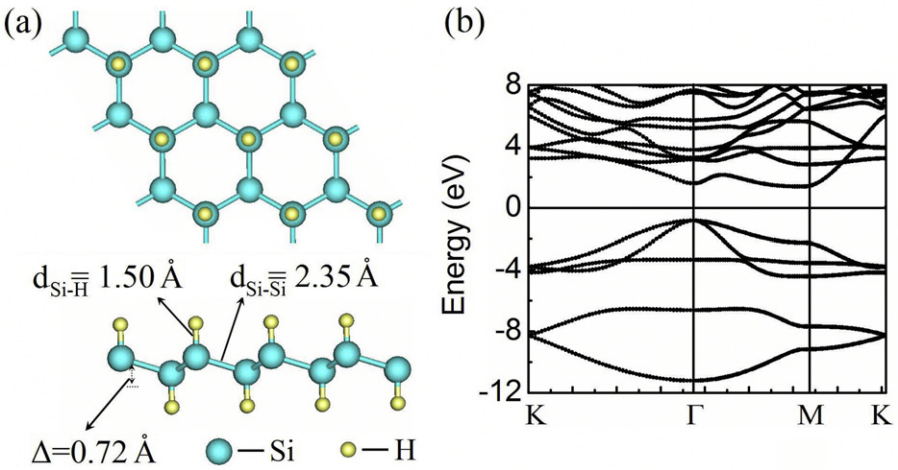

Fig. 1. (a) Top and side views of silicane structure, where the buckling distance Δ and the bond lengths d_{Si-Si} and d_{Si-H} are indicated. (b) Calculated energy band structure for silicane. The Fermi level is at zero.

$4 \times 4 \times 1$ Monkhorst-Pack k-meshes. Optimal atomic positions are determined until the magnitude of the forces acting on all atoms becomes less than 0.05 eV/Å. In addition, noncollinear magnetism with spin–orbit interaction is included in our calculations [39].

3. Results and discussions

We begin with the silicane structure shown in Fig. 1(a). Similar to graphane, the system can be derived by the adsorption of a H atom to each Si atom alternating between the top and bottom side in the honeycomb structure. The calculated buckling distance Δ indicated in Fig. 1(a) is 0.72 Å, which is significantly larger than that of graphane (0.45 Å) [21] and silicene (0.44 Å) [26]. This is reasonable since Si prefers the sp^3 rather than the sp^2 hybridization. Fig. 1(b) plots the band structure of silicane where the primitive cell containing two Si and two H atoms is used in the calculations. In contrast to the semi-metallic silicene [26], we see that silicane is semiconducting with an indirect band gap of 2.21 eV. The valence band maximum appears at the Γ point while the conduction band minimum at the M point. Our calculated results agree well with that found previously [31]. It is interesting to note that the carbon counterpart (graphane) has a direct band gap of 3.42 eV [21]. On the other hand, our spin-polarized calculations find that silicane is nonmagnetic.

To create hydrogen vacancies on the surface of silicane, one can use various techniques such as laser beam resonating with surface–hydrogen bond [40] and stripping with ionic vapor [41]. Due to the dangling bond of unsaturated Si atom, we find that a single hydrogen vacancy created on the nonmagnetic honeycomb structure surface yields a net magnetic moment of 1 μ_B. This can be attributed to the polarization of the unpaired electrons caused by the under-coordination-induced densely, deeply, and locally entrapped bonding electrons, as observed in both the graphene [42] and ZnO [43] containing defects. If there are two hydrogen vacancies arranged as the nearest neighbor in the honeycomb structure, the system is found to be nonmagnetic because of π–π pairing of the two unsaturated Si atoms. When the two hydrogen vacancies are farther away from each other, the system becomes magnetic (ferromagnetic or antiferromagnetic) since the π–π interaction between the two unsaturated Si atoms will vanish.

We now discuss the magnetic moment attained in a domain of hydrogen vacancies. Fig. 2 shows some examples with single-sided hydrogen vacancies in the honeycomb structure. Here we label the domain as L_n^s, T_n^s or H_n^s, where L, T, and H correspond to the lane, triangular, and hexagonal domain, respectively. The superscript s indicates that the domain is single-sided, while the subscript n represents the number of Si atoms at one edge. Compared with that of silicane, our calculations find that single-sided hydrogen vacancies only lead to very small changes of the relaxed structures. Moreover, the spins of unsaturated Si atoms in the single-sided domain are all ferromagnetically ordered, which is in good agreement with Lieb's theorem [44]. For a lane domain L_3^s where the H atoms attached to the three Si atoms located at the edge are all removed, we see from Fig. 2(a) that the spin density is mainly located at the three unsaturated Si atoms which yield a net magnetic moment of 3 μ_B. For a triangular domain specified as T_2^s, we see from Fig. 2(b) that the spins of three unsaturated Si atoms at the corner are parallel and induce a net magnetic moment of 3 μ_B. In the case of a hexagonal domain H_2^s shown in Fig. 2(c), we see there are totally seven H atoms removed from one side which gives a total magnetic moment of 7 μ_B. Summarizing our results, we find that the magnetic moment of single-sided domain is only determined by the total number of unsaturated Si atom (each contributes a magnetic moment of 1 μ_B) and does not depend on the geometry of the domain. Such finding is very different from that of graphane [21] where the magnetic moment is determined by both the size and shape of a domain. For the single-sided domain in graphane, H atoms tend to relocate in order to pair the spins of adjacent C atoms to form π-bonds which give a vanished magnetic moment. Nevertheless, we do not observe the relocation of H atoms for the domain in silicane, which is again due to the fact that Si atom prefers the sp^3 hybridization. On the other hand, we have considered a half-hydrogenated silicene, the unit cell of which contains two Si atoms and only one of them is passivated by H atom. Such special configuration corresponds to the largest domain of single-sided hydrogen vacancies on the surface. Our calculations indicate that the energy of the ferromagnetic (FM) state is 11 meV/cell lower than that of the antiferromagnetic (AFM) state and each unit cell carries a magnetic moment of 1 μ_B.

The magnetic moment can be also attained in the domain of double-sided hydrogen vacancies. As shown in Fig. 3, all the H atoms within a given domain are removed from silicane. Unlike that in the single-sided domain, we find that the buckled structures in the double-sided domain tend to be flattened upon geometry optimization. On the other hand, the spin of the unsaturated Si atom on the top side is found to be opposite to that on the bottom side. For a lane domain labeled as L_3^d, the three spins are thus AFM ordered and the net magnetic moment is 1 μ_B, which is also confirmed by the spin density plot shown in Fig. 3(a). It should be mentioned that if a lane domain has even number of unsaturated Si atoms, the system becomes nonmagnetic due to the entirely paired

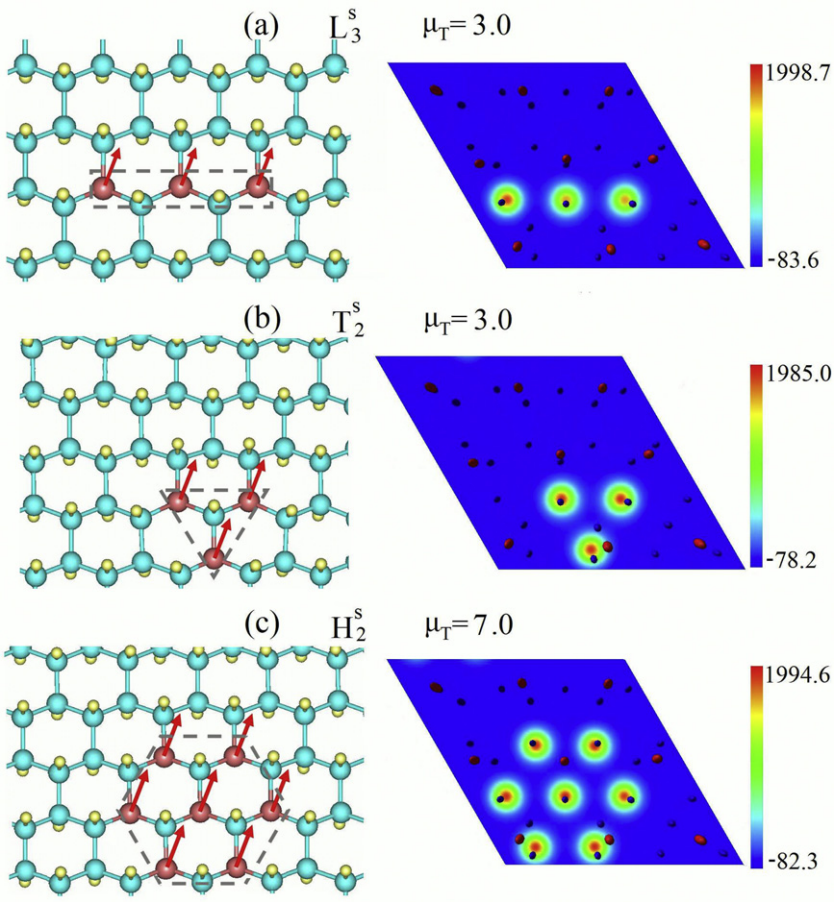

Fig. 2. The configuration of single-sided domain and the corresponding spin density plot for (a) L_3^s, (b) T_2^s, and (c) H_2^s. The total magnetic moment of each system is indicated. Note the red balls indicate unsaturated Si atoms and other atoms are just the same as those shown in Fig. 1.

π-orbitals. In the triangular domain T_2^d shown in Fig. 3(b), there are three unsaturated Si atoms on the top side and one on the bottom side which gives a net magnetic moment of 2 μ_B. It should be mentioned there is a significant contraction of the Si—Si bond inside the domain (from 2.35 Å to 2.26 Å), and is associated with the polarization of the unpaired electrons discussed above. Similar findings are observed in other domains of vacancy. As can be seen from Fig. 3(c), the net magnetic moment of the rectangular domain R_2^d is zero since there is equal number of unsaturated Si atoms on the top and bottom side and the spin of each other is cancelled. In general, the total magnetic moment of a double-sided hydrogen vacancies domain can be given by $\mu_T = (N_t - N_b)\mu_B$, where N_t and N_b represent the number of removed H atoms from the top and bottom side, respectively. We have also considered the domain containing both single-sided and double-sided hydrogen vacancies and having arbitrary shape (not shown here). We find that the corresponding magnetic moment can be calculated as a sum of those from the single-sided and double-sided domain. Our results thus suggest that by controlling the size and/or shape of a domain, one can effectively manipulate its magnetic moment.

We now move to the electronic properties of silicane with hydrogen vacancies on its surface. For simplicity, we only consider the lane and triangular domains. Fig. 4 shows the calculated energy band structures for the above-mentioned L_3^s, L_3^d, T_2^s and T_2^d domains. Note the spin–orbit interaction is included in the calculations and there is only one set of energy bands. We see that all of them remain semiconducting and the overall topology can be roughly derived by folding the band structure of silicane shown in Fig. 1(b). Due to the creation of hydrogen vacancies on the surface and the associated polarization of the unpaired electrons, however, we observe additional flat bands (shown as red lines) around the Fermi level. Note that similar result was found previously in the graphene [42] and ZnO [43] systems. As a result, the corresponding band gaps become smaller compared with that of silicane. Detailed analysis of Fig. 4 indicates that the number of flat bands below the Fermi level equals to that above the Fermi level, which is closely related to the corresponding magnetic moment and can be simply calculated as μ_T/μ_B. For example, both the L_3^s and T_2^s domain exhibit a total magnetic moment $\mu_T = 3\,\mu_B$, and there are 3 flat bands both below and above the Fermi level as shown in Fig. 4(a) and (c). It should be mentioned that some of them are degenerated. The magnetic moments attained in double-sided domains L_3^d and T_2^d are 1 μ_B and 2 μ_B, and we see from Fig. 4(b) and (d) that the corresponding numbers of flat bands are 1 and 2 (doubly degenerate), respectively. Such correlation suggests that the flat bands around the Fermi level are induced by the unsaturated Si atoms in the domain.

Fig. 5 plots the calculated band gap of the lane and triangular domains as a function of domain size n, where both the single-sided and double-sided hydrogen vacancies are considered. We do not consider hexagonal and rectangular domains since the corresponding calculations with larger n is immense within the limit of our computation resources. As can be seen from Fig. 5, all the considered systems remain semiconducting. If we focus on the single-sided hydrogen vacancies, it is interesting to note that both the lane (L_n^s) and triangular domains (T_n^s) exhibit a band gap of about 1.0 eV and there is little change with the domain size n. This is however not the case for the double-sided hydrogen vacancies, where the band gap depends on both the shape and size of

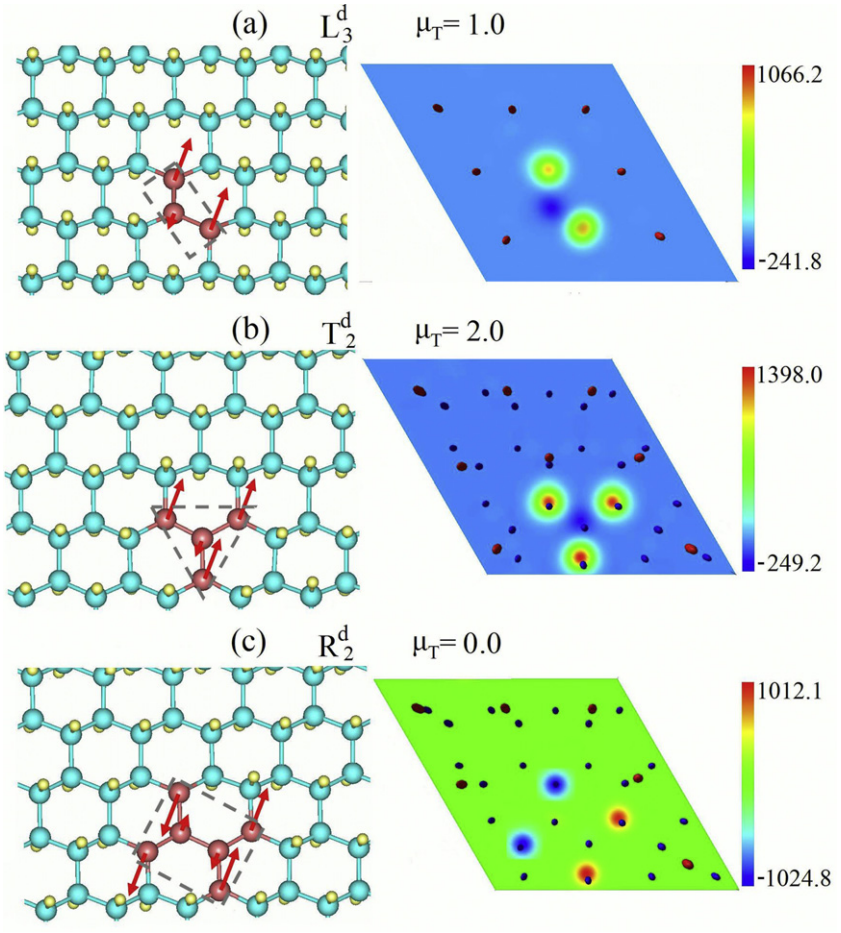

Fig. 3. The configuration of double-sided domain and the corresponding spin density plot for (a) L_3^d, (b) T_2^d, and (c) R_2^d. The total magnetic moment of each system is indicated. Note the red balls indicate unsaturated Si atoms and other atoms are just the same as those shown in Fig. 1.

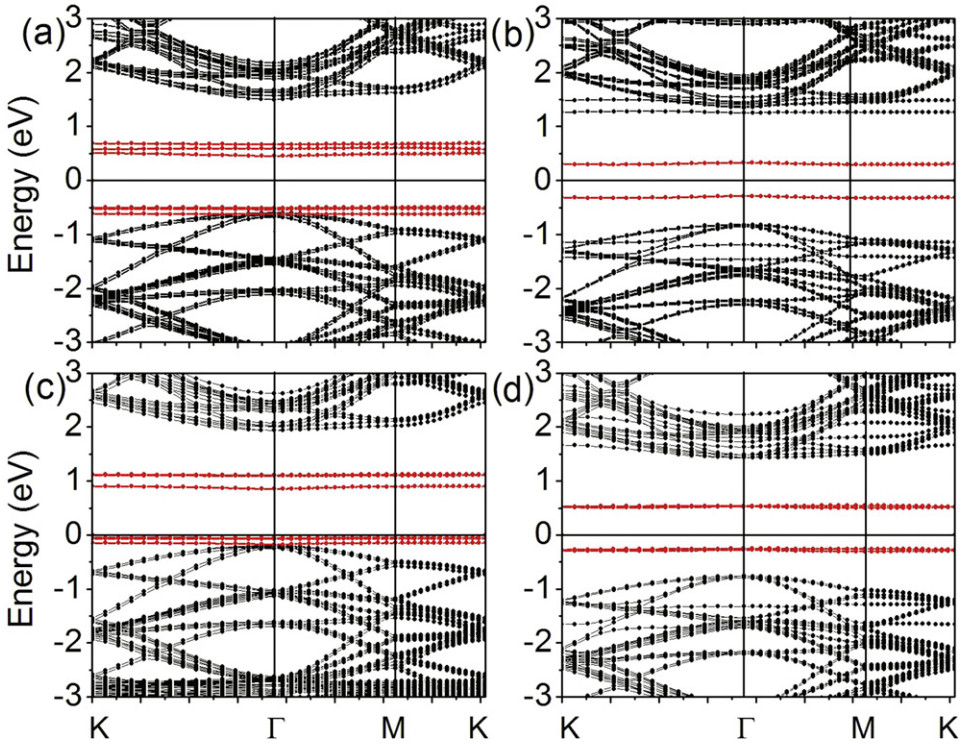

Fig. 4. The calculated energy band structures for silicane with domains (a) L_3^s, (b) L_3^d, (c) T_2^s, and (d) T_2^d. The Fermi level is at zero.

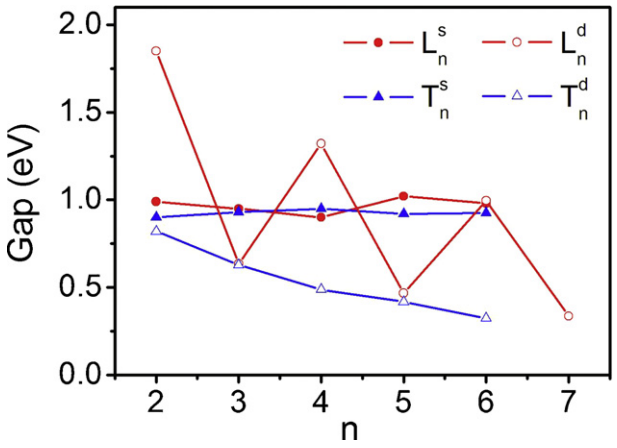

Fig. 5. The band gap as a function of domain size n for various domains L_n^s, T_n^s, L_n^d, and T_n^d.

a domain. For the lane domain L_n^d, the band gap exhibits an obvious size-dependent even-odd oscillation. If n is an even number, the unsaturated Si atoms in the domain prefer to pair adjacent π-orbitals to form maximum number of π-bonds, while there are always additional unpaired spins of Si atoms for the odd-numbered domain. According to the above discussions, the unpaired spin will induce additional flat bands around the Fermi level which tends to reduce the band gap. It is thus reasonable to expect that the band gap of odd-numbered domain is smaller than that of even-numbered one. The oscillation behavior decreases gradually with increasing domain size and can be attributed to the quantum confinement effect. For the triangular domain T_n^d, the band gap decreases monotonically as the domain size is increased. At very large n, one may expect a vanishing band gap since the system become more like a semi-metallic silicene [26].

4. Summary

In summary, our first-principles calculations indicate that controllable magnetism can be obtained by dehydrogenation on the surface of silicane, without destroying the integrity of honeycomb structure or adsorptions of transition metal atoms. The spins of unsaturated Si atoms in the single-sided domain are ferromagnetically ordered and the magnetic moment is determined by the total number of unsaturated Si atoms. In contrast, the double-sided domain is anti-ferromagnetic and the corresponding magnetic moment can be given by the difference between the number of unsaturated Si atoms on the top side and that on the bottom side. The creation of hydrogen vacancies on the silicane surface induces additional flat bands in the original band structure, and the number of which is closely related to the corresponding total magnetic moment. Moreover, the band gap can be manipulated by changing the size and/or shape of a certain domain. Due to the rich magnetic and electronic properties, the hydrosilicon honeycomb structure with hydrogen vacancies may have potential applications in future nano-scale magnetic and electronic devices.

Acknowledgements

This work was supported by the "973 Program" of China (Grant No. 2007CB607501), the National Natural Science Foundation (Grant No. 51172167), and the Program for New Century Excellent Talents in University. We also acknowledge financial support from the interdiscipline and postgraduate programs under the "Fundamental Research Funds for the Central Universities". All the calculations were performed in the PC Cluster from Sugon Company of China.

References

[1] K.S. Novoselov, A.K. Geim, S.V. Morozov, D. Jiang, Y. Zhang, S.V. Dubonos, I.V. Grigorieva, A.A. Firsov, Science 306 (2004) 666.
[2] K.S. Novoselov, A.K. Geim, S.V. Morozov, D. Jiang, M.I. Katsnelson, I.V. Grigorieva, S.V. Dubonos, A.A. Firsov, Nature (London) 438 (2005) 197.
[3] N.M.R. Peres, F. Guinea, A.H.C. Neto, Physical Review B 73 (2006) 195411.
[4] A.K. Geim, K.S. Novoselov, Nature Materials 6 (2007) 183.
[5] H. Sevinçli, M. Topsakal, E. Durgun, S. Ciraci, Physical Review B 77 (2008) 195434.
[6] A.H. Castro Neto, F. Guinea, N.M.R. Peres, K.S. Novoselov, A.K. Geim, Reviews of Modern Physics 81 (2009) 109.
[7] Y.-W. Son, M.L. Cohen, S.G. Louie, Physical Review Letters 97 (2006) 216803.
[8] D.E. Jiang, B.G. Sumpter, S. Dai, Journal of Chemical Physics 126 (2007) 134701.
[9] F.J. Owens, Journal of Chemical Physics 128 (2008) 194701.
[10] B. Xu, J. Yin, Y.D. Xia, X.G. Wan, K. Jiang, Z.G. Liu, Applied Physics Letters 96 (2010) 163102.
[11] V.M. Pereira, F. Guinea, J.M.B. Lopes dos Santos, N.M.R. Peres, A.H. Castro Neto, Physical Review Letters 96 (2006) 036801.
[12] J.J. Palacois, J. Fernanández-Rossier, L. Brey, Physical Review B 77 (2008) 195428.
[13] M.P. Lopez-Sancho, F. de Juan, M.A.H. Vozmediano, Physical Review B 79 (2009) 075413.
[14] Y.C. Chang, S. Hass, Physical Review B 83 (2011) 085406.
[15] D.C. Elias, R.R. Nair, T.M.G. Mohiuddin, S.V. Morozov, P. Blake, M.P. Halsall, A.C. Ferrari, D.W. Boukhvalov, M.I. Katsnelson, A.K. Geim, K.S. Novoselov, Science 323 (2009) 610.
[16] J.O. Sofo, A.S. Chaudhari, G.D. Barber, Physical Review B 75 (2007) 153401.
[17] D.V. Boukhvalov, M.I. Katsnelson, A.I. Lichtenstein, Physical Review B 77 (2008) 035427.
[18] J. Zhou, M.M. Wu, X. Zhou, Q. Sun, Applied Physics Letters 95 (2009) 103108.
[19] R. Balog, B. Jørgensen, L. Nilsson, M. Andersen, E. Rienks, M. Bianchi, M. Fanetti, E. Lægsgaard, A. Baraldi, S. Lizzit, Z. Sljivancanin, F. Besenbacher, B. Hammer, T.G. Pedersen, P. Hofmann, L. Hornekær, Nature Materials 9 (2010) 315.
[20] D. Haberer, D.V. Vyalikh, S. Taioli, B. Dora, M. Farjam, J. Fink, D. Marchenko, T. Pichler, K. Ziegler, S. Simonucci, M.S. Dresselhaus, M. Knupfer, B. Büchner, A. Grüneis, Nano Letters 10 (2010) 3360.
[21] H. Şahin, C. Ataca, S. Ciraci, Applied Physics Letters 95 (2009) 222510.
[22] C.K. Yang, Carbon 48 (2010) 3901.
[23] J. Berashevich, T. Chakraborty, Nanotechnology 21 (2010) 355201.
[24] Y. Zhang, Y.W. Tan, H.L. Stormer, P. Kim, Nature 438 (2005) 201.
[25] E. Durgun, S. Tongay, S. Ciraci, Physical Review B 72 (2005) 075420.
[26] S. Cahangirov, M. Topsakal, E. Aktürk, H. Şahin, S. Ciraci, Physical Review Letters 102 (2009) 236804.
[27] H. Şahin, S. Cahangirov, M. Topsakal, E. Bekaroglu, E. Aktürk, R.T. Senger, S. Ciraci, Physical Review B 80 (2009) 155453.
[28] S.Q. Wang, Physical Chemistry Chemical Physics 13 (2011) 11929.
[29] Z.Y. Ni, Q.H. Liu, K.C. Tang, J.X. Zheng, J. Zhou, R. Qin, Z.X. Gao, D.P. Yu, J. Lu, Nano Letters 12 (2012) 113.
[30] B. Lalmi, H. Oughaddou, H. Enriquez, A. Kara, S. Vizzini, B. Ealet, B. Aufray, Applied Physics Letters 97 (2010) 223109.
[31] L.C. Lew Yan Voon, E. Sandberg, R.S. Aga, A.A. Farajian, Applied Physics Letters 97 (2010) 163114.
[32] M. Houssa, E. Scalise, K. Sankaran, G. Pourtois, V.V. Afanas'ev, A. Stesmans, Applied Physics Letters 98 (2011) 223107.
[33] T.H. Osborn, A.A. Farajian, O.V. Pupysheva, R.S. Aga, L.C. Lew Yan Voon, Chemical Physics Letters 511 (2011) 101.
[34] J.C. Garcia, D.B. de Lima, L.V.C. Assali, J.F. Justo, Journal of Physical Chemistry C 115 (2011) 13242.
[35] G. Kresse, J. Hafner, Physical Review B 47 (1993) 558.
[36] G. Kresse, J. Hafner, Physical Review B 49 (1994) 14251.
[37] G. Kresse, J. Furthmüller, Computation Materials Science 6 (1996) 15.
[38] J.P. Perdew, Y. Wang, Physical Review B 45 (1992) 13244.
[39] D. Hobbs, G. Kresse, J. Hafner, Physical Review B 62 (2000) 11556.
[40] Z. Liu, L.C. Feldman, N.H. Tolk, Z. Zhang, P.I. Cohen, Science 312 (2006) 1024.
[41] L. Breaux, B. Anthony, T. Hsu, S. Banerjee, A. Tasch, Applied Physics Letters 55 (1989) 1885.
[42] X. Zhang, Y.G. Nie, W.T. Zheng, J.L. Kuo, C.Q. Sun, Carbon 49 (2011) 3615.
[43] J.W. Li, S.Z. Ma, X.J. Liu, Z.F. Zhou, C.Q. Sun, Chemical Reviews 112 (2012) 2833.
[44] E.H. Lieb, Physical Review Letters 62 (1989) 1201.